PROCEEDINGS of the
23rd International Congress on Acoustics
9 to 13 September 2019 in Aachen, Germany

Radiation optimization of piezoelectric plates

Olivier DOARÉ, Emil GARNELL, Corinne ROUBY

[(1)]IMSIA, ENSTA Paristech, France, {olivier.doare,emil.garnell,corinne.rouby} ensta-paristech.fr

Abstract

The goal of the present work is to control the modal dynamics of a piezo-electric loudspeaker in order to reach directivity of efficiency criteria. In this context, we study the dynamics and sound radiation of a piezoelectric plate biased by a static pressure on one side. This pressure inflates the plate and its forced dynamics around this equilibrium position are then studied. With the help of von Karman plate theory, the static equilibrium position of a plate of arbitrary shape is sought for before writing its linear dynamics around this equilibrium position. This two-step problem is solved numerically using a finite elements software (Freefem++). This results in a series of eigenmodes and eigenfrequencies for each value of the static pressure difference. Next the modal forces due to the piezoelectric coupling are calculted. By considering a baffled plate, the acoustical radiation is computed using the Rayleigh integral. The numerical model is used to perform a parametric optimisation of the system.

Keywords: Piezoelectic plates, Loudspeaker, Optimisation, Genetic algorithm, Radiation

1 INTRODUCTION

Numerous studies have focused on the dynamics of piezoelectric plates, with the aim of designing loudspeakers [4], reducing the acoustic transmission through panels [9], or controlling structural vibrations [2]. Often, a Kirchhoff-Love linear plate model taking into account piezoelectric coupling is considered [8]. An antisymmetric configuration of the piezoelectric layers is then considered in order to couple the electric field and the bending moments within the plate. Conversely, a symmetrical configuration produces only membrane forces and therefore does not allow to generate a transverse displacement of the plate in the context of this linear modeling. To couple the electric field to the transverse displacement in this context, the structure must have a curvature. It is then necessary to consider shells or prestressed plates. We propose here a plate configuration prestressed by a pressure differential on which we can vary the degree of asymmetry of the piezoelectric layers.

Although this system can have many applications (sensors for non-destructive testing, microphone, energy harvesting...), we focus here on a speaker-type application and wish to optimize the radiation of the system. One of our objectives is to find a configuration with a response to an electrical signal dominated by the response of a single mode of vibration, over the widest possible frequency range, by adjusting the shape of the electrodes glued on the piezoelectric plate. There are several works in the literature seeking to achieve a modal forcing by playing on the shape of the electrodes [5, 4, 10]. The approach developed in the present article will use the same principles by integrating the prestresses, the degree of asymmetry and the acoustic radiation properties at low frequencies into optimization.

First, we will derive a model of a piezoelectric plate prestressed by a static pressure differential and dynamically excited by an electric voltage on the electrodes. This model will next be used to optimize various parameters in order to create a system radiating in a single structural mode. Finally, some optimization results will be presented and analyzed.

2 PIEZOELECTRIC PLATE MODEL

We are interested in the system represented on figure 1. The piezoelectric plate has a thickness h and an arbitrary shape of characteristic dimension L. This plate consists of a linear and isotropic elastic material, char-

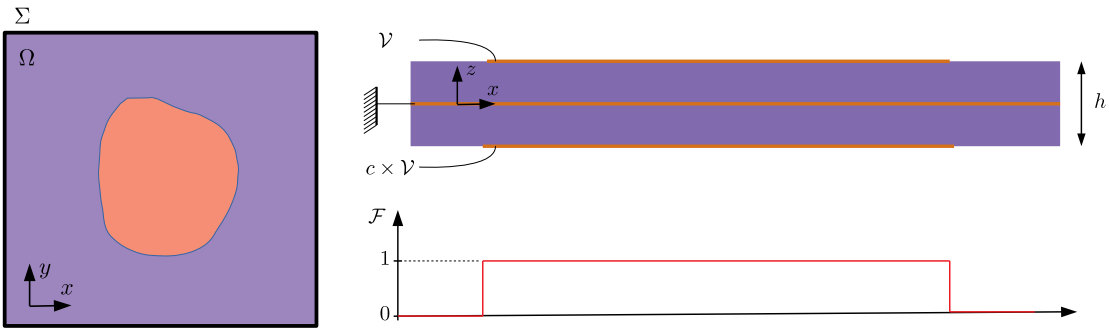

Figure 1. Schematic view of the problem : a plate defined by the border Σ where it is clamped. The interior domain is denoted Ω. The plate consists of two piezoelectric layers separated by an electrode. Upper and lower layers are partially covered by an electrode, indicated by the orange color. The electrical potentials are $\mathscr{V}$ and $c\mathscr{V}$ on the upper and lower layers respectively.

acterized by its Young modulus E and Poisson's ratio ν. The edge of the plate is denoted Σ. The displacement is written $\underline{\xi} = u\underline{e}_x + v\underline{e}_y + w\underline{e}_z$. The equations describing the dynamics of this plate are obtained from the assumptions of Von Kármán [6] (thin plate, w at most of h and small derivatives in front of the unit, small deformations, Kirchhoff's assumptions for the stresses in the median plane, and small in-plane displacements u and v compared to w).

Locally, the stresses in the plate are the sum of internal stresses due to the deformation and the stresses generated by the piezoelectric coupling:

$$\begin{aligned}
\sigma_{xx} &= \frac{E}{1-\nu^2}(\varepsilon_{xx} + \nu\varepsilon_{yy}) + e_{31}\mathscr{F}\mathscr{E} \\
\sigma_{yy} &= \frac{E}{1-\nu^2}(\varepsilon_{yy} + \nu\varepsilon_{xx}) + e_{31}\mathscr{F}\mathscr{E} \\
\sigma_{xy} &= \frac{E}{1+\nu}\gamma_{xy}
\end{aligned} \tag{1}$$

where $\mathscr{E}$ is the electric field along z. The latter equals $2\mathscr{V}/h$ in the upper half and $2c\mathscr{V}/h$ in the lower half. It is assumed here that the piezoelectric coupling is only between the electric field along z and the uniaxial stresses in the plane of the plate, and that this coupling is isotropic in the plane. In equations (1), e_{31} is the associated piezoelectric coupling coefficient. The function $\mathscr{F}$ is a function that describes the fact that electrodes partially corver the piezoelectric film. This factor equals 1 where the electrode is present, and 0 elsewhere.

The equations describing the nonlinear dynamics of the system taking into account the Von Kármán hypotheses set out above are detailed in numerous works (for example [1]). The same development is carried out here taking into account the piezoelectric coupling as introduced in equation (1). After introducing the membrane forces N_x, N_y, N_{xy}, and the moments M_x, M_y, M_{xy}, the behavior equations link these six generalized forces to deformations through six equations written below in dimensionless form, using the following quantities for the scaling:

$$\text{Time: } L^2\sqrt{\frac{\rho(1-\nu^2)}{Eh^2}} \qquad \text{Lengths: } L \qquad \text{Pressure: } \frac{Eh^3}{12(1-\nu^2)L^3} \tag{2}$$

$$\text{Membrane stresses: } \frac{Eh}{1-\nu^2} \qquad \text{Moments: } \frac{Eh^3}{12L(1-\nu^2)} \qquad \text{Voltage: } \frac{Eh}{e_{31}(1-\nu^2)} \tag{3}$$

The mechanical behaviour writes:

$$N_x = \frac{\partial u}{\partial x} + \nu \frac{\partial v}{\partial y} + \frac{1}{2}\left(\frac{\partial w}{\partial x}\right)^2 + \frac{\nu}{2}\left(\frac{\partial w}{\partial y}\right)^2 + (1+c)\mathscr{F}v, \tag{4}$$

$$N_y = \frac{\partial v}{\partial y} + \nu \frac{\partial u}{\partial x} + \frac{1}{2}\left(\frac{\partial w}{\partial y}\right)^2 + \frac{\nu}{2}\left(\frac{\partial w}{\partial x}\right)^2 + (1+c)\mathscr{F}v, \tag{5}$$

$$N_{xy} = \frac{1-\nu}{2}\left[\frac{\partial u}{\partial y} + \frac{\partial v}{\partial x} + \frac{\partial w}{\partial x}\frac{\partial w}{\partial y}\right], \tag{6}$$

$$M_x = -\frac{\partial^2 w}{\partial x^2} - \nu \frac{\partial^2 w}{\partial y^2} + 3l(1-c)\mathscr{F}v, \tag{7}$$

$$M_y = -\frac{\partial^2 w}{\partial y^2} - \nu \frac{\partial^2 w}{\partial x^2} + 3l(1-c)\mathscr{F}v, \tag{8}$$

$$M_{xy} = -(1-\nu)\frac{\partial^2 w}{\partial x \partial y}, \tag{9}$$

and equilibrium writes:

$$\frac{\partial N_x}{\partial x} + \frac{\partial N_{xy}}{\partial y} = 0, \tag{10}$$

$$\frac{\partial N_{xy}}{\partial x} + \frac{\partial N_y}{\partial y} = 0, \tag{11}$$

$$p + \ddot{w} + \frac{\partial^2 M_x}{\partial x^2} + \frac{\partial^2 M_y}{\partial y^2} + 2\frac{\partial^2 M_{xy}}{\partial x \partial y} + 12l^2\left(N_x \frac{\partial^2 w}{\partial x^2} + N_y \frac{\partial^2 w}{\partial y^2} + 2N_{xy}\frac{\partial^2 w}{\partial x \partial y}\right) = 0. \tag{12}$$

These equations depend only on four dimensionless parameters: the Poisson's ratio ν, the aspect ratio $l = L/h$, the dimensionless pressure differential p and the piezoelectric forcing symmetry parameter c, in addition to eventual parameters describing the shape of the plate. The clamped edge Σ, where the outgoing normal is denoted $\underline{n}$ imposes:

$$u = v = w = 0 \quad \text{and} \quad \underline{\text{grad}}\, w \,.\, \underline{n} = 0 \quad \text{on} \quad \Sigma. \tag{13}$$

3 Linear dynamics around an equilibrium state

We are interested in the response of the system subjected to a static pressure p_0 when a voltage $\mathscr{V}(t)$ is imposed. The nonlinear equations presented in the previous section are first separated between a permanent part and low amplitude fluctuations. Order two quantities are then neglected and the weak form of the system is written to implement the finite element method with Freefem++ [7].

The nonlinear static problem of a membrane subject to $p = p_0$ is first solved. Numerically, a gradient method is implemented in Freefem++ to reach the nonlinear solution. This solution is represented in figure 2 for some typical values of the parameters.

Next, the linear dynamics of the system around the nonlinear static equilibrium resulting from the static inflation pressure p is calculated. In practice, the finite element method is used to calculate the mass and stiffness matrices M and K. It should be noted that the finite element stiffness matrix is not symmetric and the numerical modal analysis of the problem then involves two families of modes: the right modes ϕ, resulting from the direct eigenvalue problem, and the left modes ψ, given by the transposed eigenvalue problem. Thus the dynamics of the forced system in the modal basis involves an expansion along the right modes of the nine quantities of the problem. In particular, the displacement along z writes

$$w(x,y,t) = \sum_{n=1}^{N} q_n(t)\phi_{wn}(x,y), \tag{14}$$

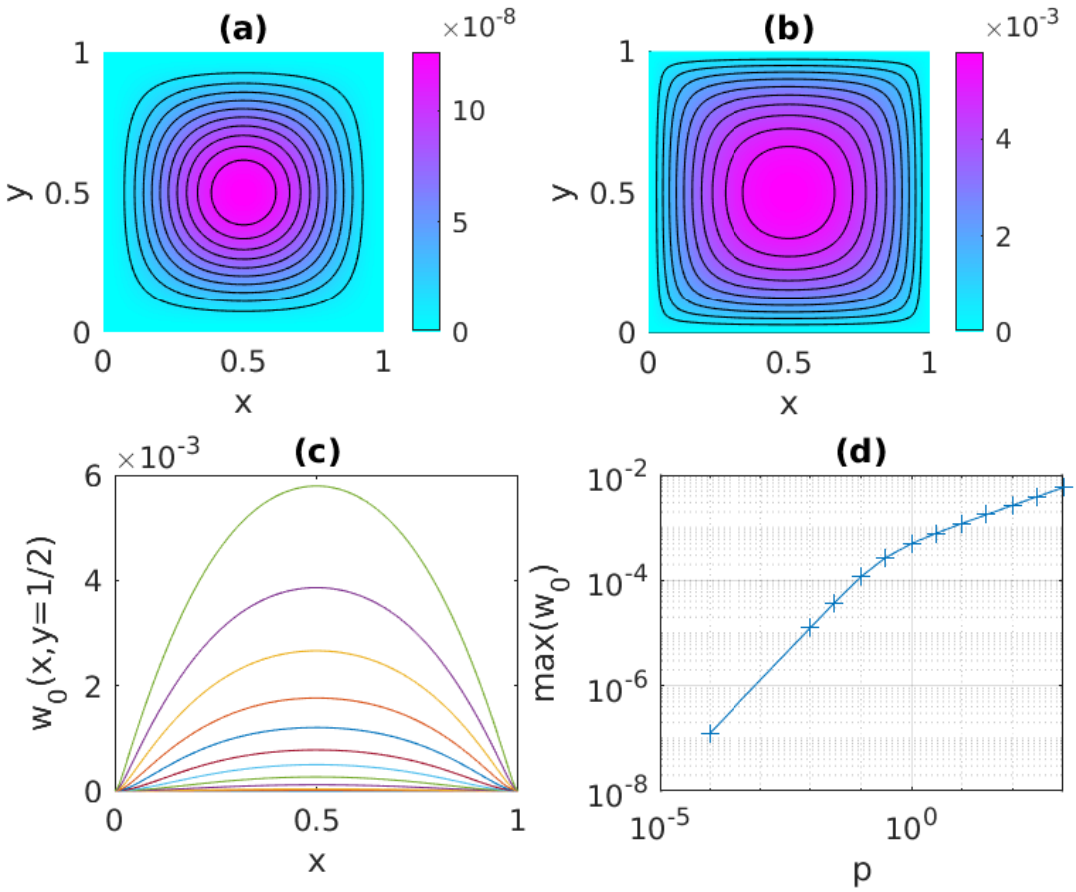

Figure 2. Static deformation of a plate submitted to a pressure differential p for $l = 3.33 \times 10^4$ and $\nu = 0.25$. (a) Displacement w for $p = 10^{-4}$, (b) displacement w for $p = 100$, (c) displacement $w(x, y = 1/2)$ for different values of p in the range $[10^{-4}, 10^3]$, (d) maximum value of w as function of p.

where the w subscript indicates that the eigenmode for w is considered. The n^{th} component of the vector of the modal forces resulting from a projection on the left modes writes:

$$F_n = \int_\Omega \left[(1+c)(\psi_{N_x n} + \psi_{N_y n}) + 3l(1-c)(\psi_{M_x n} + \psi_{M_y n})\right] \mathscr{F} v \mathrm{d}\Omega.$$

In this expression of the modal force the projections of $\mathscr{F}$ on two modal functions appear: one is related to the membrane forces $N_x + N_y$, the other to the moments $M_x + M_y$. It should be noted the the projection on the moment is scaled by the aspect ratio l. For thin plates, l is very large ($l = 3.33 \times 10^4$ in the case presented in this article). Thus, for the membrane forces to contribute significantly to the modal force n, $\psi_{N_x n} + \psi_{N_y n}$ must be several orders of magnitude greater than $\psi_{M_x n} + \psi_{M_y n}$. This is what is observed in practice for large values of the pressure p. This is illustrated in figure 3 where ϕ_{w1}, $\psi_{M_x 1} + \psi_{M_y 1}$ and $\psi_{M_x 1} + \psi_{M_y 1}$ are plotted for two inflation pressures. We observe that when p increases, the membrane forces of this mode become very large compared to the moments, so even if moments are in factor of a coefficient $l = 3.33 \times 10^4$, membrane forces are dominant.

Let $w = \Re(\hat{w}(x,y)\mathrm{e}^{\mathrm{i}\omega t})$ be the harmonic response of the plate when an input voltage of the form $v = \Re(\hat{v}\mathrm{e}^{\mathrm{i}\omega t})$

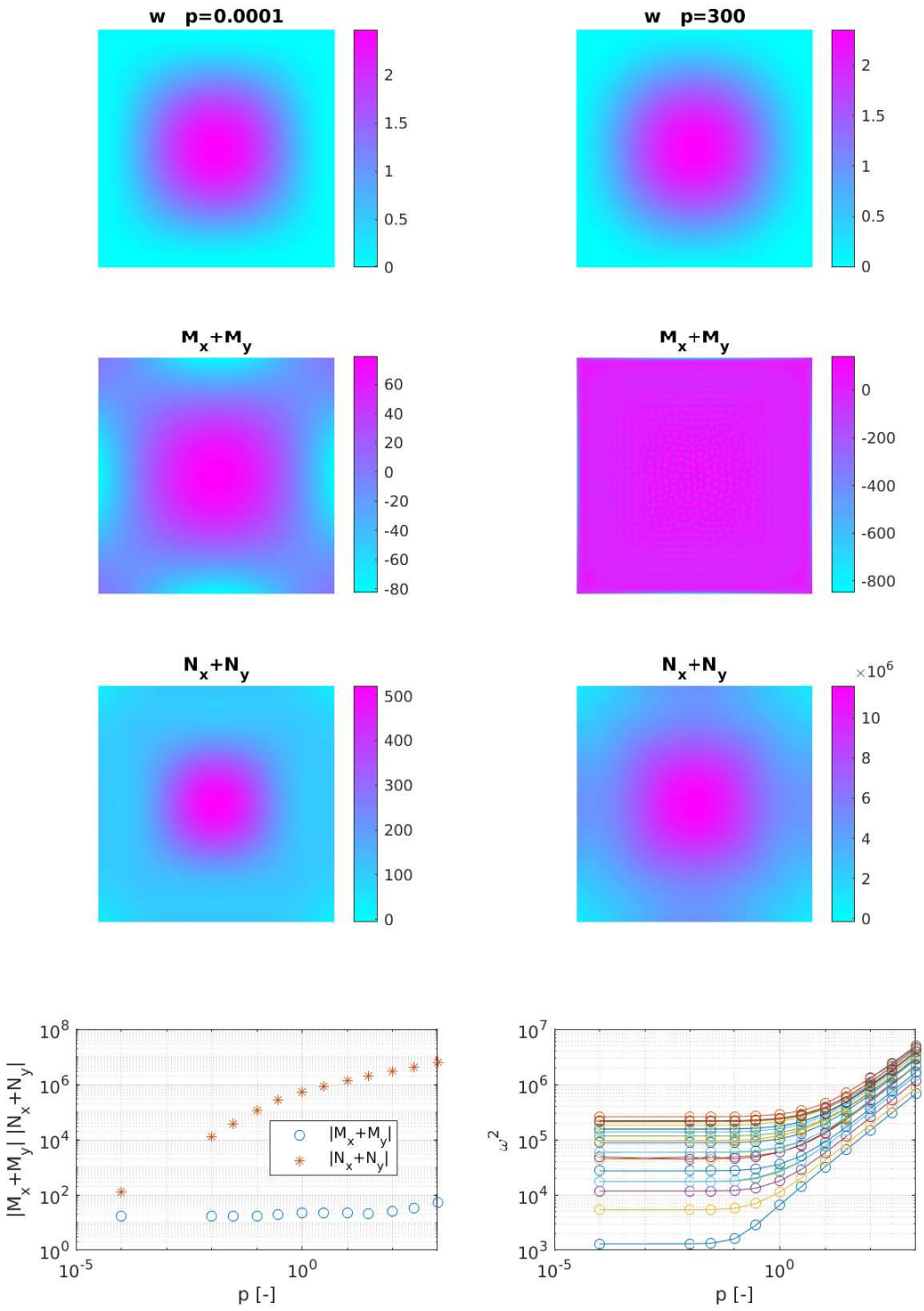

Figure 3. First eigenmode for two different pressures. The displacement of the first right mode is plotted on the first line. The membrane stresses and moments of the first left mode are plotted on the second and third lines respectively. The mean value of these quatities and the eigenfrequencies are plotted as function of p on the down-left and down-right figures respectively.

is applied. The amplitude in the Fourier space $\hat{w}$ then takes the form of a sum of modal contributions,

$$\hat{w}(x,y) = \sum_n \frac{F_n \phi_{wn}(x,y)}{\omega_n^2 - \omega^2 - 2i\eta\omega_n\omega}. \tag{15}$$

In the above equation η is an arbitrary linear constant damping, which is added for consistency to take into account different sources of damping in the mechanical system. Experiments on real systems would be necessary to correctly model the damping. Assuming that radiated acoustic wavelengths are large compared to L, the pressure P (in pascals) radiated at a distance $R_0 \gg L$ from the embedded plate in an infinite rigid plane takes the simple form below,

$$\frac{2\pi P}{\rho_f c_0^2} = -e^{ikr_0} \sum_n \frac{F_n \chi_n}{\omega_n^2 - \omega^2 - 2i\eta\omega_n\omega}, \quad \text{with } \chi_n = \int_\Omega \phi_{wn} ds, \tag{16}$$

where k is the acoustic wave number adimensioned by L and $r_0 = R_0/L$. This low frequency approximation is the monopole radiation approximation, obtained in practice from the Rayleigh integral [3]. We thus see that with the approximations made above, the contribution to the radiation of a mode n of the structure is directly proportional to the product $F_n\chi_n$. Hence, the optimization of the following section is based on this particular quantity.

4 Optimisation of the electrodes' geometry

The radiation associated with an input voltage $v(t)$ of the system has been calculated in the previous section. This modeling can then be used to optimize the geometry of the system for different purposes. We propose here to work on a geometry of electrodes defined from concentric rings, parametrized by five rays and plotted in figure 4abc. This geometry defines the function $\mathscr{F}$ represented in figure 1 and appearing in the equation (15), which is 1 where the electrode is present and 0 elsewhere. The goal here is to maximize the radiation of the plate of one mode m, and minimize the other modes radiation. We thus seek to minimize the cost function:

$$J = \frac{\sum_{n=1, n\neq m}^{N} (\chi_n F_n)^2}{(\chi_m F_m)^2}, \tag{17}$$

with the following constraints

$$0 < r_1 < r_2 < r_3 < r_4 < r_5 < \frac{1}{2} \quad \text{and} \quad -1 < c < 1. \tag{18}$$

This optimization was performed for different values of the parameters l, ν and p using a genetic algorithm implemented under Matlab. In the following we will focus on the case $m = 1$.

In figure 4 are presented three cases of best local optima for three different inflation pressures. The frequency response functions far from the plate are also plotted in figure 4. The shaded lines correspond to the frequency response obtained if we make an error of $+5\%$ or -5% on the dimensions of the electrodes. The plate subjected to a high inflation pressure seems both to give a more robust optimum and to increase the efficiency of the radiation.

5 Conclusion

We presented a weakly nonlinear model of a plate of arbitrary shape forced by a static pressure differential and by a dynamic loading by piezoelectric coupling. This model allows a quick calculation of the dynamics and the acoustic radiation and could thus be used to optimise several parameters (electrode geometry $r_1 ... r_5$ and asymmetry coefficient of the piezoelectric forcing c) in order to maximize the radiation of one mode compared to the others. This optimization problem has many local minima and although a long phase of exploration of the

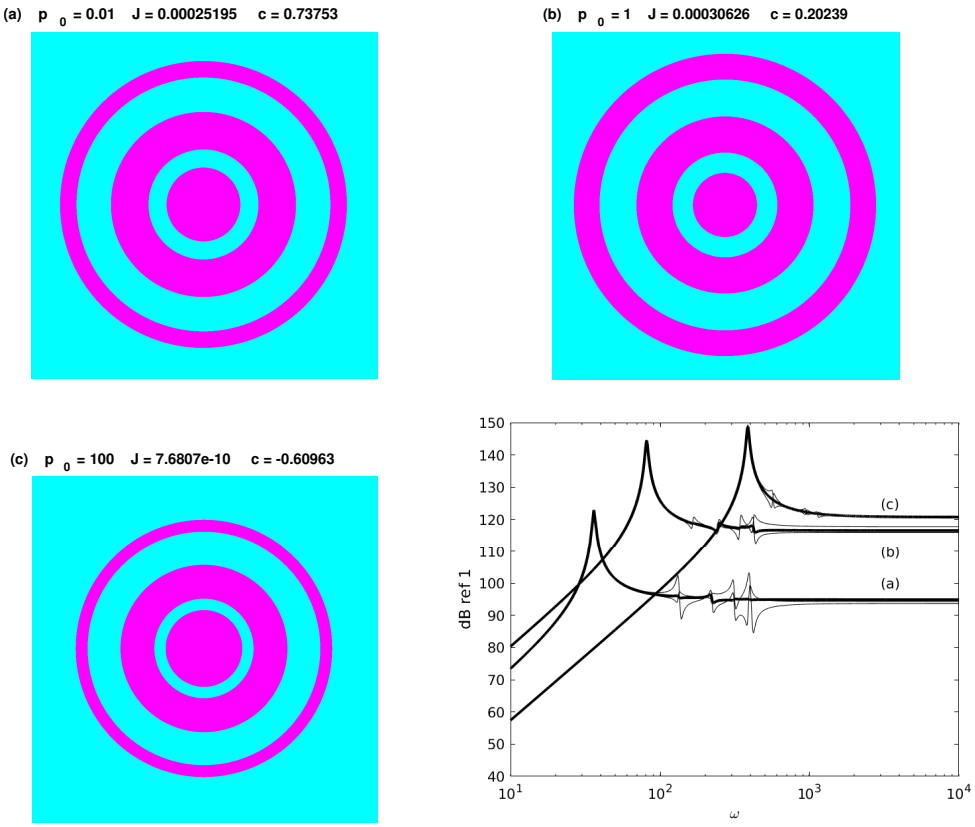

Figure 4. Various electrode shapes (local minima of J) found by the genetic algorithm. Pink corresponds to $\mathscr{F} = 1$, blue corresponds to $\mathscr{F} = 0$.

genetic algorithm with large populations is done for each case, we have no evidence that the global minimum. However, the results show that we are able to isolate the radiation of a single mode.

We also note a very high sensitivity of the cost function J to the parameters of the problem, the minimum found by the genetic algorithm, whether local or global, lies at the bottom of a very narrow well. This feature is not mentioned in previous work on actuators or modal sensors based on a binary elecrode distribution ($\mathscr{F} = 0$ or 1) [5], and can cause reliability problems in a practical application. The configuration proposed in this work can advantageously overcome this problem, because two parameters can be adjusted after the design of the device, the inflation pressure p_0 and the asymmetry coefficient c of the piezoelectric forcing.

We are now working on other forms and other optimization objectives, as well as on the realization of optimized prototypes.

References

[1] M. Amabili. *Nonlinear vibrations and stability of shells and plates*. Cambridge University Press, 2008.

[2] I. Bruant, L. Gallimard, and S. Nikoukar. Optimal piezoelectric actuator and sensor location for active vibration control, using genetic algorithm. *Journal of Sound and Vibration*, 329(10):1615–1635, 2010.

[3] A. Chaigne and J. Kergomard. *Acoustique des Instruments de Musique*. 2008.

[4] O. Doaré, G. Kergourlay, and C. Sambuc. Design of a circular clamped plate excited by a voice coil and piezoelectric patches used as a loudspeaker. *Journal of Vibration and Acoustics*, 135(5):051025, 2013.

[5] A. Donoso and J. C. Bellido. Distributed piezoelectric modal sensors for circular plates. *Journal of Sound and Vibration*, 319(1-2):50–57, 2009.

[6] Y. C. Fung. *Foundations of solid mechanics(Book on deformation and motion of elastic and plastic solids including variational calculus and tensor analysis)*. Englewood Cliffs, N. J., Prentice-Hall, Inc. edition, 1965.

[7] F. Hecht and A. le Hyaric. http://www.freefem.org/ff++/index.htm.

[8] C. K. Lee. Theory of laminated piezoelectric plates for the design of distributed sensors actuators .1. Governing equations and reciprocal relationships. *Journal Of The Acoustical Society Of America*, 87:1144–1158, 1990.

[9] N. Quaegebeur, P. Micheau, and A. Berry. Decentralized harmonic control of sound radiation and transmission by a plate using a virtual impedance approach. *J. Acoust. Soc. Am.*, 125(5):2978–86, 2009.

[10] X. Zhang and Z. Kang. Topology optimization of piezoelectric layers in plates with active vibration control. *Journal of Intelligent Material Systems and Structures*, 25(6):697–712, 2014.